DENTAL MATERIALS 35 (2019) 585–596

Available online at www.sciencedirect.com

ScienceDirect

journal homepage: www.intl.elsevierhealth.com/journals/dema

# Real-time in-depth imaging of gap formation in bulk-fill resin composites

*Juri Hayashi*[a,b], *Jorge Espigares*[b], *Tomohiro Takagaki*[b], *Yasushi Shimada*[c], *Junji Tagami*[b], *Tomoko Numata*[d], *Daniel Chan*[a], *Alireza Sadr*[a,b,*]

[a] *Department of Restorative Dentistry, Biomimetics Biomaterials Biophotonics Biomechanics & Technology Laboratory, School of Dentistry, University of Washington, 1959 NE Pacific Street, Seattle, WA 98195-7456, USA*
[b] *Cariology and Operative Dentistry, Department of Restorative Sciences, Graduate School of Medical and Dental Sciences, Tokyo Medical and Dental University, 1-5-45, Yushima, Bunkyo-ku, Tokyo 113-8549, Japan*
[c] *Department of Operative Dentistry, Graduate School of Medicine, Dentistry and Pharmaceutical Sciences, Okayama University, 2-5-1 Shikata-cho, Kita-ku, Okayama 700-8525, Japan*
[d] *Analytical Technology Center, Horiba Techno Service Co., Ltd., 2-6 Awaji-cho, Kanda, Chiyoda-ku, Tokyo 101-0063, Japan*

ARTICLE INFO

*Article history:*
Received 22 September 2018
Received in revised form
29 January 2019
Accepted 30 January 2019

*Keywords:*
Degree of conversion
Polymerization
Composite resins
Dental restoration failure
Optical coherence tomography
Bulk-filled
Self-cured
Shrinkage

ABSTRACT

*Objectives.* This study visualized in real-time the gap forming of bulk-fill resin composites during polymerization using optical coherence tomography (OCT).
*Methods.* Light-cured bulk-fill resin composites; Tetric N-ceram Bulk Fill (TNB), SonicFill (SNF), Surefil SDR (SDR), dual-cured bulk-fill resin composite Bulk EZ (BEZ), and light-cured core resin composite Clearfil Photo Core (CPC) were investigated. Swept-source OCT real-time cross-sectional monitoring was obtained during resin composite placement and curing procedure. Gap formation was observed in bonded cylindrical resin composite molds (4-mm depth, 3-mm diameter) and free shrinkage volume was observed at the top and bottom of a tube with similar dimensions (n = 10). OCT 3D data were analyzed to calculate sealing floor area percentage (SFA%) and volumetric shrinkage in bonded tube (VS%). Data were analyzed by ANOVA at significance level of 0.05. The bottom-top degree of conversion ratio (DC%-R) through 4-mm depth was measured using the XploRA Plus micro-Raman spectroscopy.
*Results.* BEZ showed no gap formation at the cavity floor in any specimens while SNF showed the highest gap formation; the statistical order in terms of SFA% was BEZ ($100 \pm 0$) > TNB ($84.97 \pm 2.98$) > CPC ($52.13 \pm 8.23$) = SDR ($45.97 \pm 9.21$) > SNF ($16.23 \pm 6.00$) ($p < 0.05$). On the other hand, total VS% was statistically ordered as BEZ ($3.40 \pm 0.14$) > SDR ($3.22 \pm 0.09$) > TNB ($1.82 \pm 0.11$) > SNF ($1.65 \pm 0.04$) = CPC ($1.56 \pm 0.04$) ($p < 0.05$). Unlike BEZ, the light-cured resin composites showed larger shrinkage at specimen bottom than top. TNB showed the lowest DC%-R followed by SNF ($p < 0.05$).
*Significance.* Light-cured bulk-fill resin composites showed various degrees of gap formation and shrinkage at 4-mm deep cavity. The dual-cured bulk-filled resin composite showed

* *Corresponding author at*: Department of Restorative Dentistry, University of Washington, 1959 NE Pacific Street Box 357456, Seattle, WA 98195-7456, USA.
E-mail address: arsadr@uw.edu (A. Sadr).
https://doi.org/10.1016/j.dental.2019.01.020

no decrease of degree of conversion through the depth and the highest cavity adaptation despite its tendency for higher volumetric shrinkage.



## 1. Introduction

Over the past several decades, resin composites have gradually been accepted as reliable restorative materials in dentistry [1,2]. Clinical and technical demands have promoted the development of bulk-fill resin composites which are indicated for single increment placement up to 4- or 5-mm depth [3,4]. According to the manufacturers, these resin composites generate lower polymerization shrinkage stress, allow higher light transmission and have adequate degree of conversion (DC). Improvements in bulk-fill resin composites have been made through modification of organic matrix, initiator and filler content, shape and size [5,6]. Volumetric shrinkage in methacrylate-based resin composite materials is unavoidably generated during polymerization due to reduction of the distance between monomers as the weak van der Waals forces between monomers are converted into covalent bonds [7]. Contraction stress is the result of polymerization shrinkage taking place under confinement caused by bonding to cavity walls or other increments. The magnitude of the stress and its distribution are affected by the matrix composition, volume, configuration (C-factor) and compliance of the cavity, and the kinetics of the polymerization reaction [8,9]. These stresses can affect the adhesive interface between the tooth and restoration and lead the interfacial gap formation [10–12] and subsequent clinical problems such as postoperative sensitivity due to movement of fluids in the dentinal tubules [13] Polymerization shrinkage stress can also lead to crack propagation and fracture of the tooth-restorative complex [14].

The physico-chemical properties of bulk-fill resin composites have been verified from a variety of perspectives [15–17]. Nevertheless, a correlation between these basic properties and the clinical performance of materials is not guaranteed [18]. An evidence-based recommendation for the clinical use of the bulk-fill materials requires well-designed clinical studies over a long time. On the other hand, laboratory studies in clinical-relevant set-up can provide useful insight into the clinical performance of these materials.

The bulk-fill resin composites are mainly marketed as low-viscosity (flowable) or regular-viscosity resin composites. Due to wear and mechanical properties, the majority of flowable bulk-fill resin composites are recommended to be placed with an additional layer of hybrid resin composite on the occlusal surface. Comparison of the internal adaptation between bulk-filled resin composites and incrementally placed conventional resin composites suggested that the incremental-fill technique produced better internal adaptation than the bulk-fill technique [19].

Recently, dual-cured bulk-fill resin composites have been marketed as paste-paste flowable materials with the aim to improve the DC through the depth of material; however, little information is available on their performance in comparison with light-cured bulk-fill resin composites.

Assessment of the sealing performance and morphological observation of interface affected by polymerization shrinkage have been commonly carried out using various light and electron microscopes [20,21]. These methods require sectioning and polishing of the specimen which may lead to increased artifacts and interfacial gap [22]. In such an observation, the outcome cannot clarify the mechanism of when or how the gap or defect generated. Optical coherence tomography (OCT) can visualize internal biological and biomaterial structures nondestructively using infrared light waves with high biological safety [23]. The effectiveness of OCT for evaluation of resin composite restoration marginal adaptation and interfacial gaps has been demonstrated [12,24,25]. The validity of the OCT imaging method for quantitative analysis has been verified by strong correlation with confocal laser scanning microscopic observation [26]. Moreover, thanks to the high-speed laser scanning, fast digital to analogue (DAC) technology and powerful 3D image processing, OCT is a unique method for real-time observation and 3D quantification of defect formation in dental resin composites [27]. In addition to defect analysis, the 3D image can be simply applicable for shrinkage volume analysis.

In this study, the momentary behavior of bulk-fill resin composites during light-curing was observed, and interfacial gap and shrinkage volume were quantified using OCT along with the DC of all tested resin composite. The null hypothesis was that there was no significant difference in gap formation, volumetric shrinkage and DC among the materials tested.

## 2. Materials and methods

### 2.1. *Specimen preparation*

A schematic drawing of the experiment is shown in Fig. 1. For observing interfacial gap formation and shrinkage behavior in confined environment, cylindrical cavities (3 mm in diameter, 4 mm in depth, C-factor = 4.98) and tubes (3 mm in diameter, 4 mm in height, C-factor = 2.67) were prepared on resin composite blocks using diamond bur (SF101CR, Shofu, Kyoto, Japan) attached to a high-speed turbine handpiece under water coolant. A silicone impression of the model was made (EXA'lence extra light body; GC America, IL, USA). Fifty standardized molds and 50 standardized tubes were duplicated by pouring and light-curing flowable resin composite (Estelite Flow Quick shade A2; Tokuyama Dental, Tokyo, Japan) into these silicone molds. The flowable resin composite was inserted and polymerized in 4 increments with 40 seconds using a halogen light curing unit with 600 mW/cm$^2$ light irradiance (Optilux 501, Kerr, Orange, CA, USA) for each increment. After the cavity preparation,

**Table 1 – Tested composites, specimen preparation and surface treatment materials used in the study.**

| Tested composites | | | |
|---|---|---|---|
| Material/Shade (Code/Lot No). Manufacturer | Type recommended light activation time and irradiance | Composition (filler wt% & vol%) | Characteristics (as claimed on the manufacturer website) |
| Tetric N-ceram Bulk fill/IVA (TNB/R52450)<br>Ivoclar Vivadent AG, Schaan, Liechtenstein | High-viscosity light-cured bulk-fill composite<br>20 s (≥500 mW/cm$^2$)<br>10 s (≥1000 mW/cm$^2$) | Monomers; Bis-GMA, Bis-EMA, UDMA<br>Fillers; Barium aluminium silicate glass, Ytterbium, Trifluoride, Prepolymer, Mixed Oxide<br>(77 wt%, 55 vol%) | Shrinkage stress: isofiller; partially functionalized by silane and lower elastic modulus, acts as a stress reliever<br>Depth of cure: ivocerin and Lucirin TPO; lower peak sensitive with high absorption coefficient, contribute to greater depth of cure up to 4 mm<br>Other features: stabilizer/inhibitor; delay the polymerization process, possible to use as a single layer |
| SonicFill/A2 (SNF/4637057)<br>Karr, Orange, CA, USA | High-viscosity light-cured bulk-fill composite<br>20 s (650 – 1000 mW/cm$^2$)<br>10 s (>1000 mW/cm$^2$) | Monomers; Bis-EMA, Bis-GMA, TEGDMA<br>Fillers; Barium glass, Silicon dioxide<br>(83.5 wt%, 69 vol%) | Shrinkage stress: lower shrinkage stress ensure marginal integrity<br>Depth of cure: refractive index matching and an enhanced curing mechanism allow up to 5 mm polymerization depths<br>Other features: rheological modifiers; increase the flowability through sonic energy as dispensed using the special hand piece, possible to use as a single layer |
| Surefil SDR/Universal (SDR/1707000776)<br>Dentply Sirona, York, PA, USA | Low-viscosity light-cured bulk-fill composite<br>20 s (550 – 1000 mW/cm$^2$)<br>10 s (1000 – 2000 mW/cm$^2$) | Monomers; SDR patented UDMA, TEGDMA, EBPDMA<br>Fillers; Barium and strontium alumino fluoro silicate glass<br>(68 wt%, 45 vol%) | Shrinkage stress: patented urethane dimethacrylate monomer with high molecular weight and lower volumetric shrinkage. Polymerization modulator; optimize flexibility and higher dissipation of energy<br>Depth of cure: allows a bulk fill of up to 4 mm<br>Other features: self-leveling feature; allow intimate adaptation to the cavity, requires additional occlusal layer |
| Bulk EZ/A2 (BEZ/41551)<br>Danville Materials, Carlsbad, CA, USA | Low-viscosity dual-cured bulk-fill composite<br>10 s (no specific recommendation for the irradiance) | Monomers; EBPDMA, TEGDMA, Bis-GMA, UDMA<br>Fillers; Fluoride compound, Glass compound<br>(Proprietary/Proprietary) | Shrinkage stress: the self-cure system with IntelliTek technology designed to specifically control and direct shrinkage, addressing the issue of stress from rapid curing<br>Depth of cure: unlimited cure depth<br>Other features: self-cure system compatible with a wide variety of bonding agents cavity adaptation; High flowablity, additional occlusal layer optional |
| Clearfil Photo Core/Universal (CPC/B20160)<br>Kuraray Noritake Dental, Tokyo, Japan | High-viscosity core build-up composite<br>40 s (Halogen, 300–550 mW/cm$^2$)<br>20 s (LED, >300 mW/cm$^2$)<br>5 s (Halogen, >550 mW/cm$^2$) | Monomers; TEGDMA, Bis-GMA<br>Fillers; Silanated silica filler, silanated barium glass filler<br>(83 wt%, 68 vol%) | Shrinkage stress: small polymerization shrinkage<br>Depth of cure: cures up to a depth of 10 mm<br>Other features: developed specifically as a core build-up material that cuts like dentin |

– Table 1 (*Continued*)

| Specimen preparation and surface treatment materials | | | |
|---|---|---|---|
| Materials Lot No. | Manufacturer | Composition | Application |
| Estelite Flow Quick shade A2 JO651 | Tokuyama Dental, Tokyo, Japan | Monomers; Bis-MPEPP, TEGDMA, UDMA, Fillers; Silica-zirconia filler, silica-titania fillers (71 wt%, 53 vol%) | Dispense in layers up to 2 mm in thickness; Light cure for 20 s |
| K-etchant gel 3D0042 | Kuraray Noritake Dental, Tokyo, Japan | 35–45% phosphoric acid, colloidal silica, water | Apply onto the adherent surface and leave for 5 s; thoroughly wash and dry |
| Clearfil Ceramic Primer Plus A50030 | Kuraray Noritake Dental, Tokyo, Japan | Methacryloxypropil trimethoxy silane, MDP, ethanol | Apply to the adherent surface; dry the entire adherent surface sufficiently using mild, oil-free air blow |
| Clearfil SE Bond 2 Bond 4R0318 | Kuraray Noritake Dental, Tokyo, Japan | MDP, Bis-GMA, HEMA, hydrophobic dimethacrylate, CQ, N,N-diethanol *p*-toluidine, silanated filler | Apply onto the adherent surface and gently air blow; light cure for 10 s |

Bis-EMA, bisphenol-A polyethylene glycol diether dimethacrylate; Bis-GMA, bisphenol-A diglycidyl ether dimethacrylate; Bis-MPEPP, bisphenol A polyethoxy methacrylate; CQ, camphorquinone; EBPDMA, ethoxylated bisphenol-A-dimethacrylate; HEMA, 2-hydroxyethyl methacrylate; MDP, 10-methacryloyloxydecyl dihydrogen phosphate; TEGDMA, triethylene glycol dimethacrylate; UDMA, urethane dimethacrylate.

it was stored in 37 °C for 1 week to complete polymerization. In order to provide sufficient bonding, the inner surfaces of the molds were sandblasted with 50 μm alumina particles (MicroEtcher II; Danville Materials, Carlsbad, CA, USA) at 0.4 MPa for 15 s, followed by ultrasonic cleaning for 10 min (Model US 102; SND, Nagano, Japan), phosphoric acid cleaning (K-etchant gel; Kuraray Noritake Dental, Tokyo, Japan), silanization (Clearfil Ceramic Primer Plus; Kuraray Noritake Dental, Tokyo, Japan) and bond application (Clearfil SE Bond 2 Bonding Agent; Kuraray Noritake Dental, Tokyo, Japan). All surface conditioning steps were performed in accordance with the manufacturer's instructions as listed in Table 1.

Five types of resin composites recommended for bulk placement in 4 mm depth were evaluated (Table 1); Two high-viscosity light-cured bulk-fill resin composites; SonicFill (SNF; Karr, Orange, CA, USA) and Tetric N-ceram Bulk Fill (TNB; Ivoclar Vivadent AG, Schaan, Liechtenstein), a low-viscosity light-cured bulk-fill resin composite; Surefil SDR (SDR; Dentply Sirona, York, PA, USA), a low-viscosity dual-cured bulk-fill resin composite; Bulk EZ (BEZ; Danville Materials, Carlsbad, CA, USA), and a high-viscosity core resin composite; Clearfil Photo Core (CPC; Kuraray Noritake Dental, Tokyo, Japan). All materials were placed in bulk and the free surfaces were covered by plastic matrix (Hawe Transparent Striproll, Kerr, Orange, CA, USA) due to flattening the surface and isolation without disturbing the light delivering. TNB and CPC were placed using a hand instrument as a single increment. SDR and BEZ were directly dispensed from the syringe using the provided nozzle. SNF was sonic activated (SonicFill handpiece, Kerr, Orange, CA, USA) to place the material with the regulating ring of the handpiece set at level 3. According to the instruction, after resin composite placement only BEZ required 90 s before starting light activation. The halogen light curing unit light guide tip was set perpendicularly as close as possible to the top surface of the placement, and employed to 40 s light-cure the resin composites irradiance of 600 mW/cm$^2$ via plastic matrix.

### 2.2. *Optical observation of interfacial gap formation and volumetric shrinkage*

A swept-source OCT system (IVS-2000; Santec, Komaki, Ehime, Japan) with a center wavelength was 1330 nm (bandwidth 110 nm) and 30-kHz sweep rate was used for evaluation of the interfacial gaps formation in the cavities and the free surface displacements at the both ends of the tube specimens. The optical resolution is 20 μm transversally and 12 μm axially in air (7–8 μm in tissues with a refractive index around 1.5). The technical details of the system have been reported previously [27]. During placement and polymerization of the resin composite in the cavities, the OCT probe was placed beneath the cavity so that the cavity floor adhesive interface could be imaged. The the XZ cross-sectional images (B-scans) were recorded continuously at the center of the cavity in real time as a windows media video file at a resolution of 800 × 600 pixels and 20 frames per second. 3D scans were obtained immediately after light-curing at 256 × 256 × 1024 pixels over an XYZ volume of 5 × 5 × 7 mm$^3$. OCT probe was then rotated 90° and the adaptation at the axial walls of all cavities was confirmed. For the resin composites placed in the tubes, 3D scans at both ends of the tubes were separately obtained as described.

### 2.3. *Quantitative 3D analysis*

Amira software (version 5.5.0, FEI Visualization Sciences Group, Oregon, USA) was used for OCT 3D data analysis. For interfacial gap quantification, a volume of interest (VOI) of 3 × 3 × 0.1 mm$^3$, covering the whole cavity floor area was selected on each scan. A binary image was created by averaging XY slices over 100-μm thick region at the floor using the maximum intensity projection (MIP) in the VOI, according to the established method [26,27]. Sealed floor area percentage (SFA%) values were calculated considering the area proportion of the binarized pixel clusters over total floor area in each MIP image.

For shrinkage volume quantification, OCT 3D data were obtained at both ends of tube immediately after light curing.

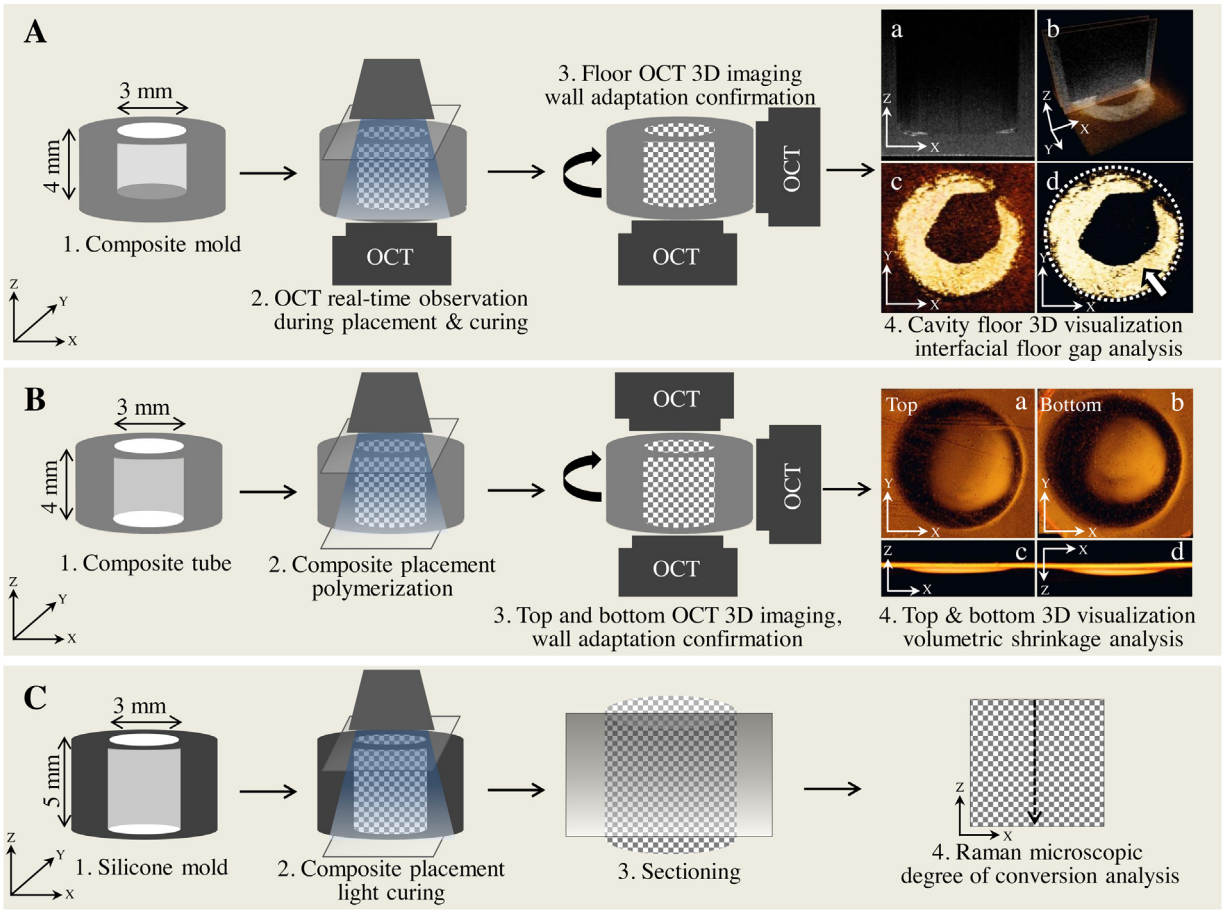


**Fig. 1 – Schematic of methodology for interfacial gap analysis (A), volumetric shrinkage analysis (B), and degree of conversion analysis (C); real-time video of OCT XZ plane image was obtained during bulk-fill resin composite placement and polymerization procedure (A2) in resin composite mold (A1). Right after curing, 3D OCT scan of the cavity floor was obtained and the wall adaptation was confirmed (A3). OCT 3D image was reconstructed by a series of OCT XZ data (A4a, b). The selected region of the cavity floor was projected on Z axis using the MIP method (A4c). The gap area percentage (blank arrow) in whole cavity area (broken line circle) was calculated (A4d). For volumetric shrinkage analysis, OCT 3D scans of the tube top and bottom were performed immediately after light-curing and the wall adaptation was confirmed (B1-3). B4a–b present *en face* and B4c–d show side views of the tube ends reconstructed in 3D by Amira software. The volumetric shrinkage percentage in whole tube volume was calculated. For degree of conversion analysis, the specimen polymerized in silicone tube with both ends covered by plastic matrix was sectioned at the center after 24 h storage (C1–3). Raman spectrums were recorded on the vertical line at the center of the cross-section (C4).**

Volumetric shrinkage percentage in bonded tube (VS%) were calculated considering the volume change at each end of the tube over the total volume of tube. The ends of tube were distinguished as the side close to the light source (top) and opposite side (bottom). The total volumetric shrinkage percentage in bonded tube (TVS%), was calculated as sum of the top-VS% and bottom-VS%.

### 2.4. *DC ratio*

Resin composites disks were placed in a silicone mold (3 mm in diameter, 5 mm in height) in the same manner as described above. After 24 h storage in dry and dark condition at 37 °C, the disks were axially sectioned at the centers with low-speed diamond saw (Isomet, Buehler, Lake Bluff, IL, USA). Raman microscopy (The XploRA Plus, Horiba, Kyoto, Japan) with power output of 5 mW was used to collect 638 nm wavelength laser spectrum along a Z-axis line at the center of the cross-section at 100 μm intervals. The intensity ratio (IR) was calculated using the phenyl CC peak at 1607 $cm^{-1}$ as an immutable reference and the vinyl CC peak at 1635 $cm^{-1}$ as a reaction peak, which would decrease with polymerization. To exclude the effect of oxygen inhibition and surface irregularities, measurements were started at 300 μm below the top surface; $IR_{Top}$ was obtained as the average of 0.3–0.7 mm from the top surface and $IR_{Bottom}$ was obtained as the average of 3.6–4.0 mm from the top surface. The bottom-to-top DC ratio (DC-R%) which means the extent of polymerization decrement through depth was calculated according to the formula:

$$DC - R\,(\%) = \frac{IRTop}{IRBottom} \times 100$$

### 2.5. *Cross-sectional microscopy*

In order to confirm the location and pattern of gap formation, direct observation of the interface in the specimen under confocal laser scanning microscopy (CLSM, 1LM21H/W; Lasertec Co., Yokohama, Japan) was accomplished after trimming the specimen to the central cross-section. The trimming was done with different sizes of SiC paper ranging from 280-grit up to 2000-grit followed by diamond pastes down to a particle size of 0.25 μm in circular motion under copious cooling water to reach vicinity of the cross-section imaged by OCT. The cavity floor on each cross-section was imaged at ×500 and ×1250 magnification.

### 2.6. *Statistical analysis*

SFA%, TVS% and DC-R% values were statistically analyzed using one-way analysis of variance. A two-way repeated-measure analysis of variance was applied to VS% values, with the free surface location (top and bottom) as the within-subjects factor and the material as the between-subjects factor. All the analyses were performed using the Statistical Package for Social Science (SPSS, Chicago, IL, USA) with the significance level set at $\alpha = 0.05$. Bonferroni correction was used for post-hoc comparisons.

## 3. Results

Still images from the OCT real-time videos are shown in Fig. 2. The representative video clips edited in Windows Movie Maker (Microsoft, Bellevue, WA) are presented in the Videos A–E. Gaps, indicated by bright lines from high signal intensities at the interface, mainly initiated from nearby the internal line angles at a few seconds after starting irradiation, and progressed toward the center of the cavity. The extent, initiation timing and propagation rates differed depending on materials (Fig. 2A–C and Videos A–C). BEZ showed no interfacial gap appearance during light curing (Fig. 2D and Video D). In TNB, CPC and BEZ, prior to appearance of the gaps, existing voids and air bubbles entrapped in resin composites showed enlargements (Fig. 2C).

In MIP images of cavity floors, TNB, CPC and SDR showed similar toroidal gap pattern while in SNF, the gap was extensively widespread and in BEZ, no gap was observed (Fig. 3A). SFA% was significantly affected by materials ($p < 0.001$). SNF showed the lowest values and the statistical order was

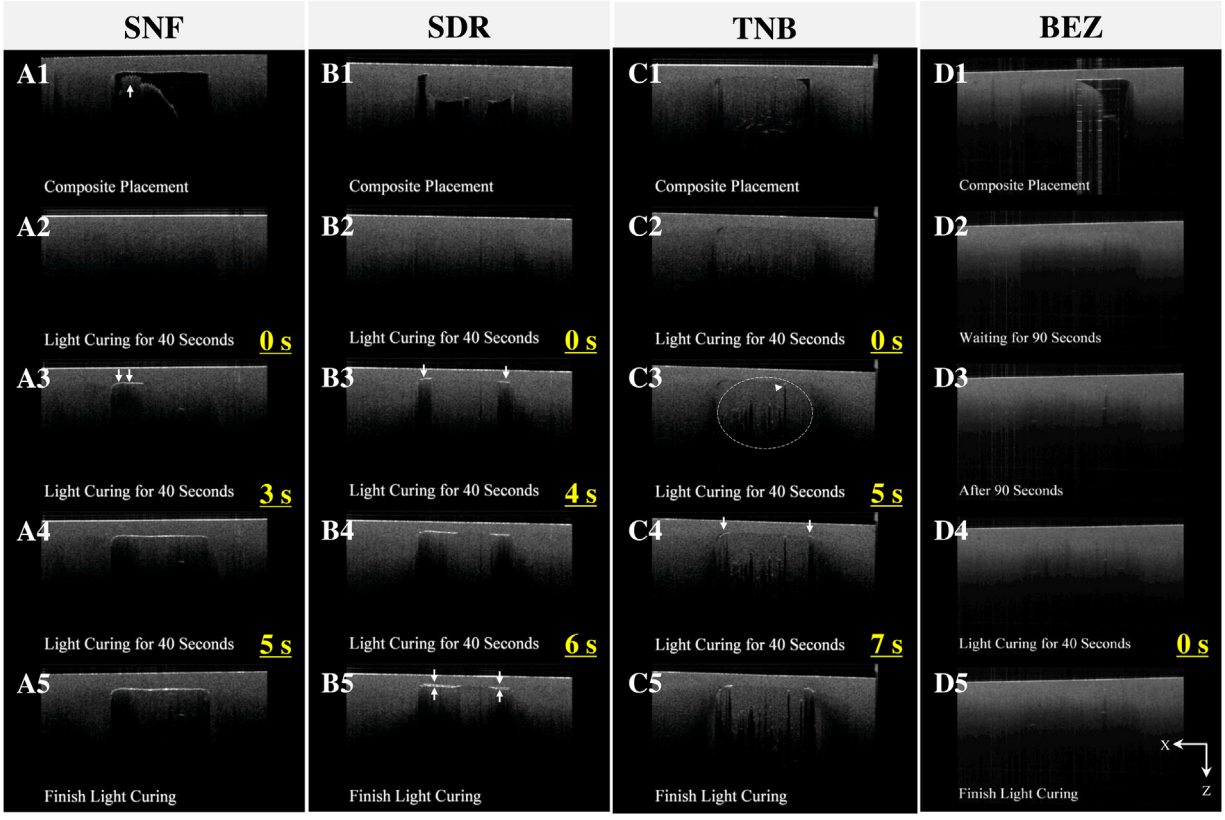


**Fig. 2 – Representative OCT B scan frames from real-time video clips during the placement and light curing procedure (A–D) replicated from each specimen at each point of time (1–5). During placement, the surface of SNF showed characteristic corrugated form due to sonic activation (A1, arrow). The high signal intensities (A3, arrows) appeared at the cavity internal angle about 3 s after starting light irradiation, and it took about 2 s for developing through the whole cavity floor (A4). In SDR, high signal intensities appeared at the both cavity corners 4 s after starting light irradiation (B3, arrows), and progressed to around 65% of the cavity floor in 2 s (B4). After the horizontal development of gaps through the floor interface stopped, the series of high signal intensities developed into the double lines indicating widening of the gap (B5, arrows). In BEZ, during the observation no high signal intensity was shown at the cavity interface (D).**

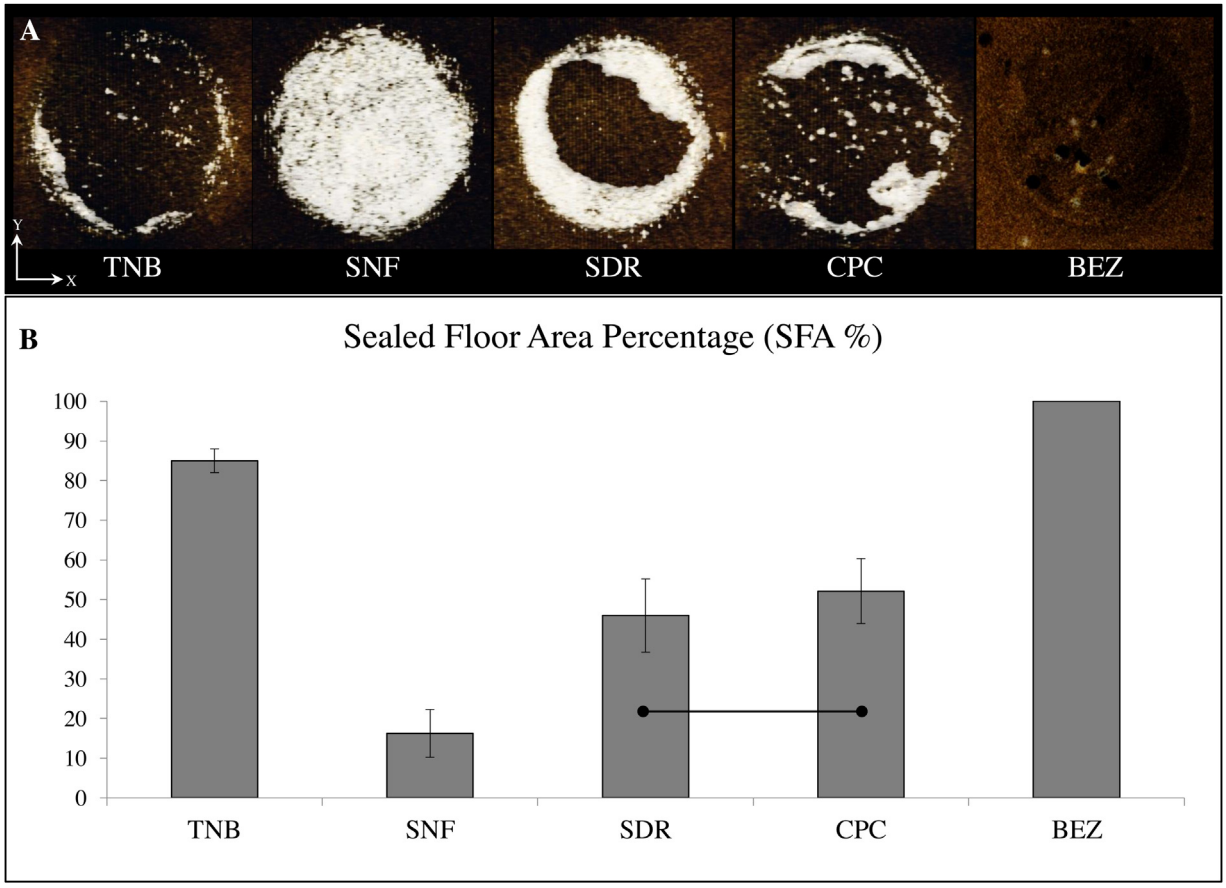


**Fig. 3 – Representative reconstructed XY plane MIP images of the cavity floors from OCT 3D data just after light curing (A). Sealed floor area percentage (SFA%) of each groups with their standard deviations (B). Horizontal bars indicate no significant differences between these groups ($p > 0.05$).**

BEZ > TNB > CPC = SDR > SNF (Fig. 3B). Representative correlative OCT and CLSM images were presented in Fig. 4. Increased signal intensity on OCT B-Scan corresponded to the gaps and bubbles in CLSM images (Fig. 4A1–A4). In a BEZ specimen with no increased OCT signal intensity, no gaps could be observed at the cavity interface under CLSM (Fig. 4A5, C). Under CLSM, most gaps were observed to be located between bulk-fill resin composites and adhesive (Fig. 4B).

Shrinkage in bonded tube test suggested that in all tested materials, polymerization shrinkage led to free surfaces deformation to form a concavity at both tube ends (Fig. 5A). VS% was significantly affected by materials and free surface locations, and the interaction was also significant ($p < 0.001$). Each light-cured material showed significantly different VS% between top and bottom surfaces ($p < 0.001$), with larger volumetric shrinkage at the bottom. On the other hand, there was no significant difference between bottom and top for BEZ ($p > 0.05$) (Fig. 5B). In terms of total shrinkage, BEZ showed the largest TVS%, and the statistical order was BEZ > SDR > TNB > SNF = CPC (Fig. 5C).

TNB showed the most inferior DC-R% (70.5%) followed by SNF (81.8%), while BEZ, CPC and SDR showed little change in DC from top to bottom (Fig. 6), with BEZ reaching 103.8% DC-R%.

## 4. Discussion

A new OCT technique for real-time visualization and analysis of gap formation and progress at resin composite interfaces has been established [27]. In this study, the technique was applied for the first time to evaluate the interfacial debonding of bulk-fill resin composite in real time. The effective imaging depth of the OCT depends on the source beam characteristics and system setup, as well as optical properties of the object. While sound human enamel is reported to have low attenuation of the near-infra red light, dentin has a more anisotropic structure and an order of magnitude larger attenuation, limiting the OCT imaging depth [28]. In this study, the simulated standard cavities were made of a resin composite commonly used in OCT experiments and known to allow at least 2-mm OCT imaging depth [26,27]. The OCT probe was placed at the bottom of the 4-mm deep resin composite to allow for effective imaging of the 0.5-mm thick cavity floor. It is noteworthy that the sand blasting surface treatment of the simulated cavity and use of a bonding agent after application of the primer with silane and 10-methacryloyloxydecyl dihydrogen phosphate (MDP) adhesive monomer promoted a strong bonding to the resin composite walls [29]. This procedure enabled comparison of gap formation among resin composites as a

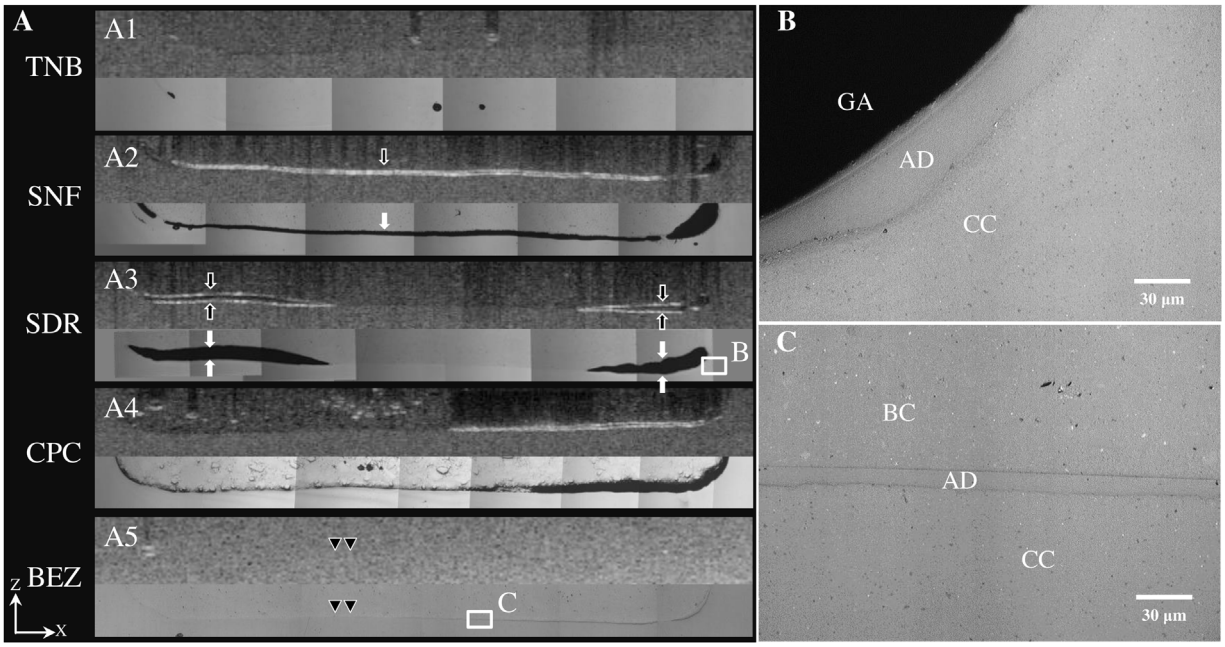


**Fig. 4 – OCT B-scan and CLSM confirmatory images obtained for each group (A) and 1250× magnification CLSM images at the corresponding areas (B, C). GA, gap; AD, adhesive; BC, bulk-fill resin composite; CC, cavity resin composite. High signal intensity (A2, blank arrow) at the cavity interface corresponds with gap (A2, bold arrow). Double bright lines (A3, blank arrows) indicated wider gaps (A3, bold arrows). High magnification CLSM image shows that the resin composite placement separates from top surface of the adhesive layer (B). Blank arrow heads are pointing toward the interface with no increase in signal intensity, indicating absence of gap as confirmed in corresponding CLSM images (A5). In confirmatory high magnification CLSM image, tight adaptation between the bulk-fill resin composite, adhesive and cavity resin composite is shown (C).**

function of polymerization kinetics and stress development at the cavity floor. Interestingly, none of the specimens showed gap formation as result of separation of the adhesive layer from the cavity wall in this study.

The compliance of cavity walls, which is characterized by the stiffness and deformation, affects stress development and distribution, cuspal deflection and interfacial gap formation [30,31]. A flowable resin composite was used to fabricate the simulated cavities in this study, which are known to lower stiffness than regular resin composites. The wall at the simulated cavity floor was much thinner than that of the axial walls (0.5 mm vs. 2 mm) allowing for higher compliance; however, no gaps were formed at the axial interfaces. In addition, the degree of conversion of the resin composite mold could have affected the results. Therefore, the use of resin composite mold instead of tooth cavity is a limitation of the current study.

This pattern of gap formation exclusively at the cavity floor is supported by previous studies tested in similar conditions of this study, which showed that large shrinkage upward-pointed vectors form at the lower part in bonded no-tapered cylindrical cavities filled by a light-cured resin composite in a single increment that could result in debonding [32,33], while this pattern due to the shrinkage vector would be potentially changed depends on the cavity shape, configuration, and adhesive conditions [33]. This shrinkage gradient through depth of placement can be explained by the light attenuation associated with the absorption and scatter within the material. When sufficient intensity of light is applied, resin composite reaches into the post-gel phase, that is, the cross-linking of the polymer chains within the resin composite increases modulus of elasticity [34]. The DC and polymerization rate of light-activated resin composite material are affected by light irradiance and exposure time [7,35]; therefore a deeper part of resin composite reaches post-gel phase at a later time compared with the shallower part i.e. adjacent to the light source. In this manner, this delay leaves room for viscous displacement at the deeper part. The results where all light-cured materials showed significantly larger volumetric shrinkage at the tube bottom than the tube top substantiated this interpretation.

Despite modifications of the formulations to improve the flexibility of the formed polymers, the light-cured materials showed various degree of gap formation at the cavity floor. The gaps initiated near the internal line angles and propagated toward the center, which corroborated that the peak stresses formed at the internal line angles of the cavity [36,37]. In addition, the nonuniform output delivered by light curing units in which generally the center of the light source shows the strongest power density [38,39] could be considered as another factors affecting the gap formation pattern.

Microfocus X-ray computed tomography (micro-CT) has been used for analysis of resin composite shrinkage patterns and volumetric shrinkage comparisons in cavities [32,40]. The OCT used in this study had comparable axial resolution with micro-CT used in previous volumetric shrinkage study (12 μm

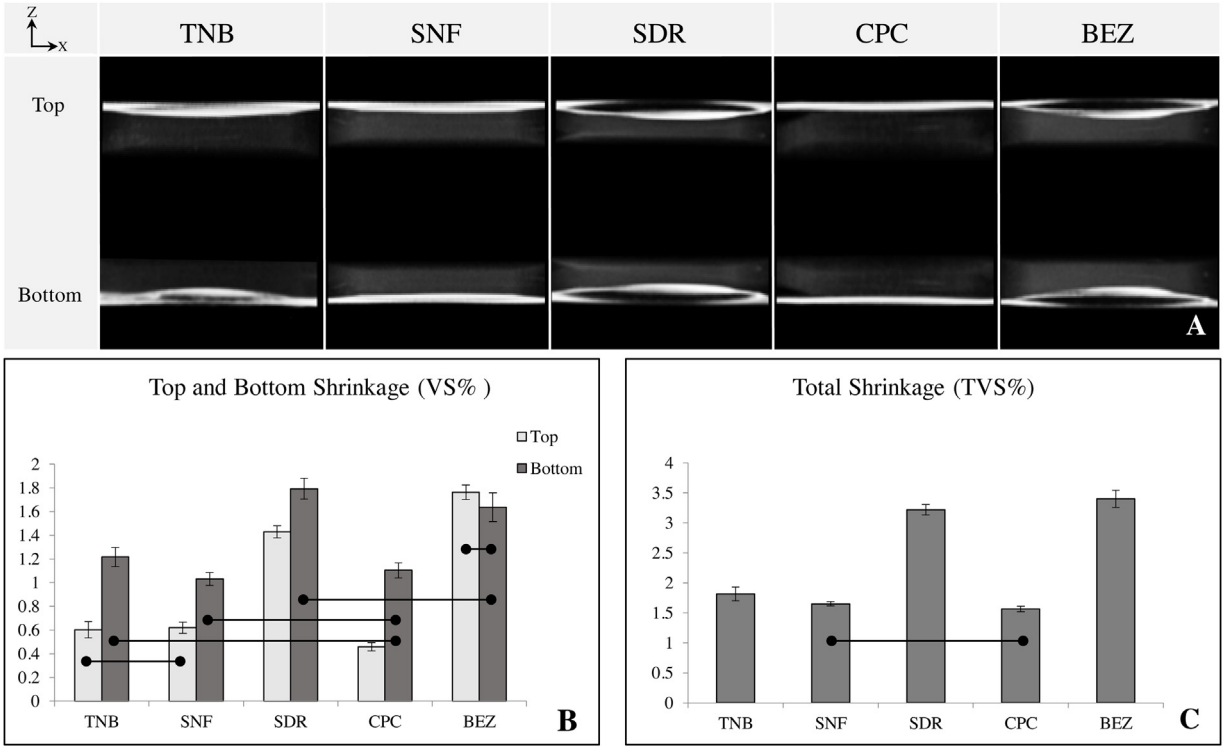


**Fig. 5 – Representative reconstructed 3D images of the top and bottom tube ends from OCT 3D data just after light curing (A). The coordinate corresponding to the imaging direction is set at the upper left corners. In all tested materials, the free surfaces deform towards the center of resin composite mass. Volumetric shrinkage percentage (VS%) and total volumetric shrinkage percentage (TVS%) of each groups with their standard deviations (B, C). A two-way repeated-measure analysis of variance was applied to VS% values and TVS% value was statistically analyzed using one-way analysis of variance. Horizontal bars indicate no significant differences between these groups ($p > 0.05$).**

in air vs. 16 μm) [40]. TVS% showed nominal values consistent with volumetric shrinkage results in the literature [41], which reported a higher shrinkage strain and stress in flowable materials compared with paste-type resin composites. In this study, the interfacial gap and volumetric shrinkage did not appear to be correlated, particularly as the dual-cured material (BEZ) showed no gap formation despite its comparable shrinkage to other flowable bulk-fill resin composite. BEZ contains a proprietary hydroperoxide oxidizing agent and a thiourea reducing agent as the catalyst redox system that allows polymerization reaction within 2 min after mixing. These catalyst systems have been reported to have similar DC but an improved shelf-life and color-stability compared with self-cured systems based on benzoyl peroxide [42]. The depth of cure in self-cure systems is not a function of light irradiance; however, slower polymerization rate [42], lower degree of cross-linking (i.e. more linear polymer) [43] and contraction stress development [44] have been reported for self-cured materials. Even though the final DC in the self-cured mode may not be necessarily lower than the dual-cured mode [43], additional light-curing would improve the polymer cross-linking [45]. In this study, it appears that the slower initial chemical polymerization reaction preceding light activation had advantages for the bulk-fill resin composite; it allowed for viscoelastic flow within the material and stress relaxation as well as for copolymerization to occur between the resin composite and adhesive at the bottom of the cavity.

Likewise, TNB showed the lowest gap formation among the light-cured materials. The DC-R% through depth was the lowest of all for this material, which could partly explain the result given that a lower DC [46] has been associated with lower stress development [47]. In addition, TNB includes proprietary germanium photo-initiator bis-(4-methoxybenzoyl)diethylgermane Ge-3 (namely Ivocerin) and phenyl propandione and acyl phosphine oxide (Lucirin TPO), which absorb relatively lower wavelength range than camphorquinone with a higher reactivity, according to the manufacturer. This together with increased inhibitor to slow the rate of polymerization and the stress [9] might have contributed to the copolymerization with adhesive at the cavity floor using the halogen light-curing source.

Several voids could be observed through the resin composites; mainly for TNB, CPC and BEZ. A previous study reported that air inclusion of between 0.1 and 2% of the total restoration volume [48]. It has been suggested that the voids can be stress relievers by increasing the material free surface, which facilitates flow during polymerization [49]. However, studies demonstrating the significance of these small voids that form unintentionally through the bulk of a dental restoration in reduction of polymerization stress are lacking.

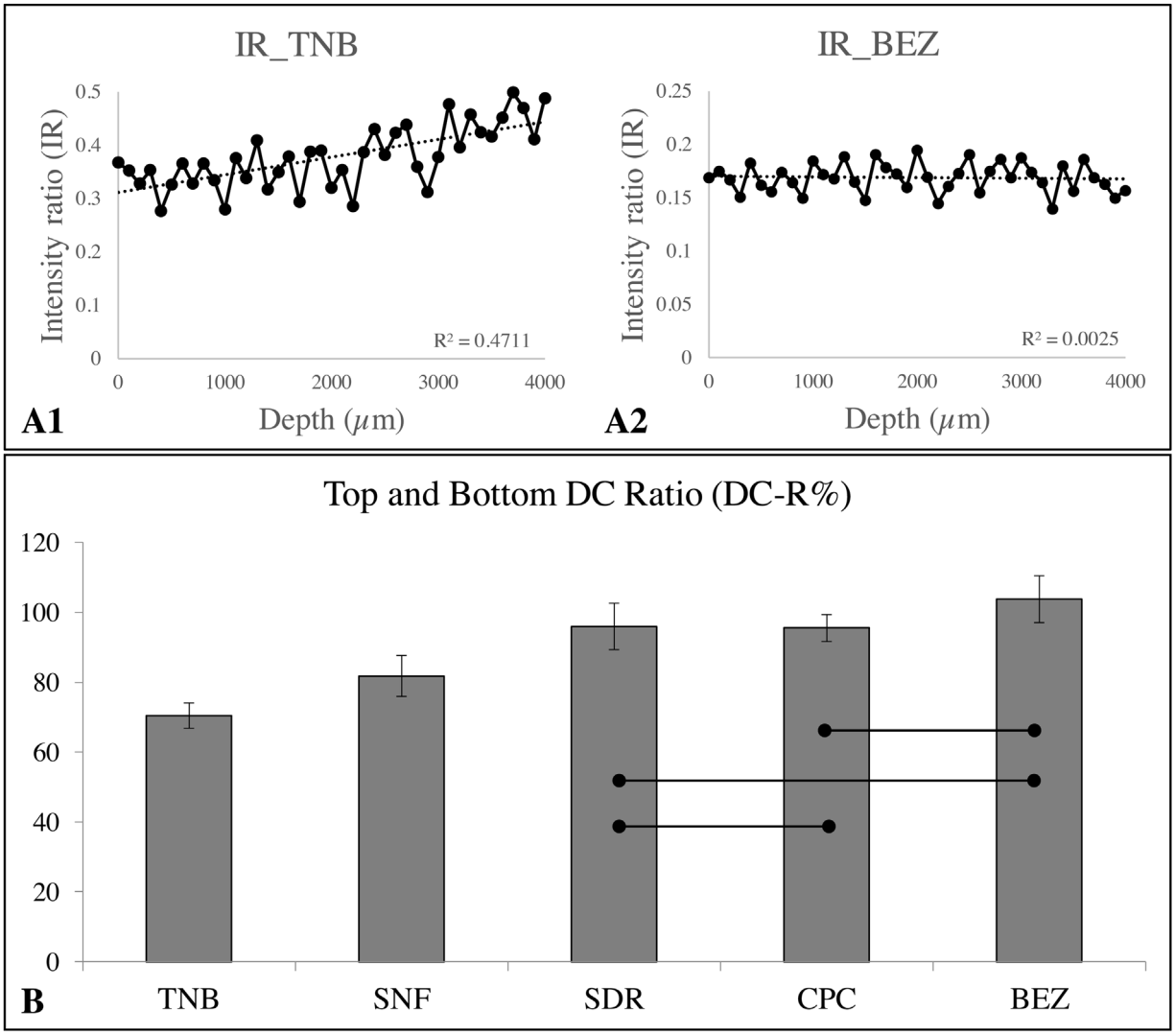


**Fig. 6 – Representative patterns of intensity ratio (IR) progression based on Raman microscopy through depth of TNB and BEZ (A1, A2). In TNB, IR shows ascending tendency, which indicates that the ratio of unreacted vinyl carbon double bonds increases at the deeper part (A1). In contrast, BEZ shows stable IR through depth (A2). DC-R% of each group with their standard deviations (B). DC-R% value was statistically analyzed using one-way analysis of variance. Horizontal bars indicate no significant differences between these groups ($p > 0.05$).**

Regarding the exent of the gap, the high-viscosity light-cured materials SNF, CPC and TNB showed different tendencies. SNF was reported to have a low light transmission through 4 mm thickness compared to other tested bulk-fill resin composites [50]. Such a significant light attenuation through SNF might have resulted in the detachment at the cavity floor interface at the early stage of light irradiation.

Lastly, the bonding quality also influences the shrinkage kinetics [32,51]. The bonding agent of Clearfil SE Bond 2 was selected for this study as an established two-step self-etch system with a water and solvent-free adhesive [26,27]. The MDP functional monomer improves bonding to various substrates and 2-hydroxyethyl methacrylate (HEMA) (Table 1) maintains integrity of the adhesive blend [26]. These monomers are found in many all-in-one or universal adhesives today, but this adhesive system was used since it polymerized better and has higher elastic modulus that its counterpart all-in-one blends [52].

It should be emphasized that the results obtained are applicable to the stricly standardized conditions underwhich the experiment was carried out. Factors such as the testing substrate, cavity configurations, bonding materials and light-curing variables could results in different outcomes. Also the interfacial integrity would be affected by long-term aging and thermomechanical loading [53]. It is expected that the OCT method will provide further insight for the research and development of improved bulk-fill resin composites.

## 5. Conclusion

OCT real-time nondestructive observation and 3D quantification were successfully applied to the bulk-fill resin composites

assessments in terms of the interfacial gap. The tested light-cured bulk-fill resin composites showed various degrees of gap formation. The dual-cured bulk-fill resin composite showed no internal gap formation and a uniform polymerization through depth, despite its tendency for higher shrinkage in the bonded tube.

## Acknowledgments

This research was supported by grants-in-aid for scientific research no. 18K17060 from the Japan Society for the Promotion of Science. The funders had no role in study conception or design, data acquisition and analysis, decision to publish, or preparation of the article.

## Appendix A. Supplementary data

Supplementary data and videos associated with this article can be found, in the online version, at https://doi.org/10.1016/j.dental.2019.01.020.

## REFERENCES

[1] Opdam NJ, Bronkhorst EM, Loomans BA, Huysmans MC. 12-year survival of resin composite vs. amalgam restorations. J Dent Res 2010;89:1063–7.
[2] Borgia E, Baron R, Borgia JL. Quality and survival of direct light-activated resin composite resin restorations in posterior teeth: a 5- to 20-year retrospective longitudinal study. J Prosthodont 2019;28:e195–203.
[3] Benetti AR, Havndrup-Pedersen C, Honore D, Pedersen MK, Pallesen U. Bulk-fill resin composites: polymerization contraction, depth of cure, and gap formation. Oper Dent 2015;40:190–200.
[4] Fronza BM, Rueggeberg FA, Braga RR, Mogilevych B, Soares LES, Martin AA, et al. Monomer conversion, microhardness, internal marginal adaptation, and shrinkage stress of bulk-fill resin composites. Dent Mater 2015;31:1542–51.
[5] Leprince JG, Palin WM, Vanacker J, Sabbagh J, Devaux J, Leloup G. Physico-mechanical characteristics of commercially available bulk-fill resin composites. J Dent 2014;42:993–1000.
[6] El-Damanhoury H, Platt J. Polymerization shrinkage stress kinetics and related properties of bulk-fill resin composites. Oper Dent 2014;39:374–82.
[7] Braga RR, Ballester RY, Ferracane JL. Factors involved in the development of polymerization shrinkage stress in resin-composites: a systematic review. Dent Mater 2005;21:962–70.
[8] Lim BS, Ferracane JL, Sakaguchi RL, Condon JR. Reduction of polymerization contraction stress for dental resin composites by two-step light-activation. Dent Mater 2002;18:436–44.
[9] Braga RR, Ferracane JL. Contraction stress related to degree of conversion and reaction kinetics. J Dent Res 2002;81:114–8.
[10] Feng L, Suh BI, Shortall AC. Formation of gaps at the filler-resin interface induced by polymerization contraction stress: gaps at the interface. Dent Mater 2010;26:719–29.
[11] Bausch JR, de Lange K, Davidson CL, Peters A, de Gee AJ. Clinical significance of polymerization shrinkage of resin composite resins. J Prosthet Dent 1982;48:59–67.
[12] Turkistani A, Nakashima S, Shimada Y, Tagami J, Sadr A. Microgaps and demineralization progress around resin composite restorations. J Dent Res 2015;94:1070–7.
[13] Opdam NJ, Roeters FJ, Feilzer AJ, Verdonschot EH. Marginal integrity and postoperative sensitivity in class 2 resin composite restorations in vivo. J Dent 1998;26:555–62.
[14] Soares CJ, Faria ESAL, Rodrigues MP, Vilela ABF, Pfeifer CS, Tantbirojn D, et al. Polymerization shrinkage stress of resin composite resins and resin cements – what do we need to know? Braz Oral Res 2017;31:e62.
[15] Lempel E, Czibulya Z, Kovacs B, Szalma J, Toth A, Kunsagi-Mate S, et al. Degree of conversion and BisGMA, TEGDMA UDMA elution from flowable bulk fill resin composites. Int J Mol Sci 2016;17.
[16] Alshali RZ, Salim NA, Satterthwaite JD, Silikas N. Post-irradiation hardness development, chemical softening, and thermal stability of bulk-fill and conventional resin-composites. J Dent 2015;43:209–18.
[17] Li X, Pongprueksa P, Van Meerbeek B, De Munck J. Curing profile of bulk-fill resin-based resin composites. J Dent 2015;43:664–72.
[18] Ferracane JL. Resin composite—state of the art. Dent Mater 2011;27:29–38.
[19] Alqudaihi FS, Cook NB, Diefenderfer KE, Bottino MC, Platt JA. Comparison of internal adaptation of bulk-fill and increment-fill resin composite materials. Oper Dent 2019;44:e32–44.
[20] Belli R, Pelka M, Petschelt A, Lohbauer U. In vitro wear gap formation of self-adhesive resin cements: a CLSM evaluation. J Dent 2009;37:984–93.
[21] Breschi L, Perdigao J, Lopes MM, Gobbi P, Mazzotti G. Morphological study of resin-dentin bonding with TEM and in-lens FESEM. Am J Dent 2003;16:267–74.
[22] Alani AH, Toh CG. Detection of microleakage around dental restorations: a review. Oper Dent 1997;22:173–85.
[23] Shimada Y, Sadr A, Sumi Y, Tagami J. Application of optical coherence tomography (OCT) for diagnosis of caries cracks, and defects of restorations. Curr Oral Health Rep 2015;2:73–80.
[24] Sadr A, Shimada Y, Mayoral JR, Hariri I, Bakhsh TA, Sumi Y, et al. Swept source optical coherence tomography for quantitative and qualitative assessment of dental resin composite restorations. Proc SPIE 2011;7884, 78840C.
[25] Bakhsh TA, Sadr A, Shimada Y, Mandurah MM, Hariri I, Alsayed EZ, et al. Concurrent evaluation of resin composite internal adaptation and bond strength in a class-I cavity. J Dent 2013;41:60–70.
[26] Bista B, Sadr A, Nazari A, Shimada Y, Sumi Y, Tagami J. Nondestructive assessment of current one-step self-etch dental adhesives using optical coherence tomography. J Biomed Opt 2013;18:76020.
[27] Hayashi J, Shimada Y, Tagami J, Sumi Y, Sadr A. Real-time imaging of gap progress during and after resin composite polymerization. J Dent Res 2017;96:992–8.
[28] Hariri I, Sadr A, Shimada Y, Tagami J, Sumi Y. Effects of structural orientation of enamel and dentine on light attenuation and local refractive index: an optical coherence tomography study. J Dent 2012;40:387–96.
[29] Spitznagel FA, Horvath SD, Guess PC, Blatz MB. Resin bond to indirect resin composite and new ceramic/polymer materials: a review of the literature. J Esthet Restor Dent 2014;26:382–93.
[30] Boaro LC, Froes-Salgado NR, Gajewski VE, Bicalho AA, Valdivia AD, Soares CJ, et al. Correlation between polymerization stress and interfacial integrity of resin composites restorations assessed by different in vitro tests. Dent Mater 2014;30:984–92.

[31] Kim YJ, Kim R, Ferracane JL, Lee IB. Influence of the compliance and layering method on the wall deflection of simulated cavities in bulk-fill resin composite restoration. Oper Dent 2016;41:e183–94.
[32] Cho E, Sadr A, Inai N, Tagami J. Evaluation of resin composite polymerization by three dimensional micro-CT imaging and nanoindentation. Dent Mater 2011;27:1070–8.
[33] Kaisarly D, El Gezawi M, Lai G, Jin J, Rosch P, Kunzelmann KH. Effects of occlusal cavity configuration on 3D shrinkage vectors in a flowable resin composite. Clin Oral Investig 2018;22:2047–56.
[34] Ferracane JL. Developing a more complete understanding of stresses produced in dental resin composites during polymerization. Dent Mater 2005;21:36–42.
[35] Sakaguchi RL, Berge HX. Reduced light energy density decreases post-gel contraction while maintaining degree of conversion in resin composites. J Dent 1998;26:695–700.
[36] Braga RR, Boaro LC, Kuroe T, Azevedo CL, Singer JM. Influence of cavity dimensions and their derivatives (volume and 'C' factor) on shrinkage stress development and microleakage of resin composite restorations. Dent Mater 2006;22:818–23.
[37] dos Santos GO, da Silva AH, Guimaraes JG, Barcellos Ade A, Sampaio EM, da Silva EM. Analysis of gap formation at tooth-resin composite resin interface: effect of C-factor and light-curing protocol. J Appl Oral Sci 2007;15:270–4.
[38] Price RB, Ferracane JL, Shortall AC. Light-curing units a review of what we need to know. J Dent Res 2015;94:1179–86.
[39] Shimokawa CAK, Turbino ML, Giannini M, Braga RR, Price RB. Effect of light curing units on the polymerization of bulk fill resin-based resin composites. Dent Mater 2018;34:1211–21.
[40] Sampaio CS, Chiu KJ, Farrokhmanesh E, Janal M, Puppin-Rontani RM, Giannini M, et al. Microcomputed tomography evaluation of polymerization shrinkage of class I flowable resin composite restorations. Oper Dent 2017;42:E16–23.
[41] Al Sunbul H, Silikas N, Watts DC. Polymerization shrinkage kinetics and shrinkage-stress in dental resin-composites. Dent Mater 2016;32:998–1006.
[42] Oei JD, Mishriky M, Barghi N, Rawls HR, Cardenas HL, Aguirre R, et al. Development of a low-color, color stable, dual cure dental resin. Dent Mater 2013;29:405–12.
[43] Meng X, Yoshida K, Atsuta M. Influence of ceramic thickness on mechanical properties and polymer structure of dual-cured resin luting agents. Dent Mater 2008;24:594–9.
[44] Feilzer AJ, de Gee AJ, Davidson CL. Setting stresses in resin composites for two different curing modes. Dent Mater 1993;9:2–5.
[45] Moosavi H, Hariri I, Sadr A, Thitthaweerat S, Tagami J. Effects of curing mode and moisture on nanoindentation mechanical properties and bonding of a self-adhesive resin cement to pulp chamber floor. Dent Mater 2013;29:708–17.
[46] Al-Ahdal K, Ilie N, Silikas N, Watts DC. Polymerization kinetics and impact of post polymerization on the degree of conversion of bulk-fill resin-composite at clinically relevant depth. Dent Mater 2015;31:1207–13.
[47] Silikas N, Eliades G, Watts DC. Light intensity effects on resin-composite degree of conversion and shrinkage strain. Dent Mater 2000;16:292–6.
[48] Nazari A, Sadr A, Shimada Y, Tagami J, Sumi Y. 3D assessment of void and gap formation in flowable resin composites using optical coherence tomography. J Adhes Dent 2013;15:237–43.
[49] Alster D, Feilzer AJ, De Gee AJ, Mol A, Davidson CL. The dependence of shrinkage stress reduction on porosity concentration in thin resin layers. J Dent Res 1992;71:1619–22.
[50] Bucuta S, Ilie N. Light transmittance and micro-mechanical properties of bulk fill vs. conventional resin based resin composites. Clin Oral Investig 2014;18:1991–2000.
[51] Chiang YC, Rösch P, Dabanoglu A, Lin CP, Hickel R, Kunzelmann KH. Polymerization composite shrinkage evaluation with 3D deformation analysis from microCT images. Dent Mater 2010;26:223–31.
[52] Sadr A, Shimada Y, Lu H, Tagami J. The viscoelastic behavior of dental adhesives: a nanoindentation study. Dent Mater 2009;25:13–9.
[53] Jung JH, Park SH. Comparison of polymerization shrinkage physical properties, and marginal adaptation of flowable and restorative bulk fill resin-based composites. Oper Dent 2017;42:375–86.